Effective, Shortened Drying of Agar-Gelcasting Al_2O_3 Tube Through Immersing in Acetone

Ramnaree Kaemkit
Prince of Songkla University
Supawan Vichaphund
National Science and Technology Development Agency (NSTDA)
Anukorn Phureungrat
Prince of Songkla University
Methee Promsawat
Prince of Songkla University
Suksawat Sirijarukul
Prince of Songkla University
Kowit Lertwittayanon (kowitpakky@yahoo.com)
Prince of Songkla University https://orcid.org/0000-0001-5121-9115

Research Article

Keywords: drying, gelcasting, agar, forming, alumina tube

Posted Date: August 26th, 2021

DOI: https://doi.org/10.21203/rs.3.rs-839902/v1

Abstract

A liquid drying agent, i.e. acetone, was employed for allowing the faster drying of Al_2O_3 tubes fabricated by agar gelcasting than the conventional air drying. The mixture of Al_2O_3 slurry and agar solution was separately prepared and then mixed prior to molding out of a set of warmed glass tubes. After the mixture transformed into gelled tube, the gelled tube was demolded and then immersed in acetone at different periods of time from 0 to 50 h. The immersed periods of 50 h led to the acetone replacement for water being inside of the gelling tube by 74 wt.% and then shortened the drying period to be 25 min. On the other hand, the conventional air drying spent 420 min drying completely. After drying, the immersed tubes possessed spherical cross section; whereas, no immersed tubes showed the deformation of cross section. The shortened drying was in line with the smaller drying shrinkage (4.7%), broader pore-size distribution and higher porous microstructure, comparing to the conventional air drying. The mechanism of acetone replacement for water was attributed to the acetone-water concentration gradient creating their inter-diffusion.

1. Introduction

The current technologies of fabricating the complex-shaped advanced ceramics have depended on the availability of sophisticated machines with high cost, for example injection molding, extrusion and isostatic pressing [1–3]. However, gelcasting method has been one of the alternative method of fabricating the complex-shaped ceramics relying on in-situ polymerization in affordable, non-porous molds such as metals, polymers and glasses [4–7]. The gelcasting method was first developed by Omatete et al during 1990s [8–10]. However, at first the polymerization needed acrylamide-based binder having neurotoxic effect for holding ceramic particles together with no deformation over a long period of drying.

Owing to the problem of neurotoxicity, the further improvement in the gelcasting method was especially focused on the low toxic-binders with the functional groups of acrylate, acrylamide, allyl and vinyl [10–14]. In addition, the binder systems of biopolymers such as agar, agarose, carrageenan and gelatin tended to be extensively adopted for forming the advanced ceramic [15–20]. However, particularly for the biopolymer-based binders, although the issue of neurotoxicity was well-tackled, their gelling strength was inadequate to maintain the same shape as the original mold. In other words, after demolding the as-gelled ceramic parts were deformable due to the conventional air drying for days relying on syneresis or the expulsion of water from gel. Moreover, the biopolymer-based gelcasting of ceramics was vulnerable to drying shrinkage due to the non-uniformity of water removal [21–23].

As a result of the drying shrinkage resulting in deformation and cracking, the new method of drying was noteworthy for solving the problem. The previous drying method included the use of liquid desiccant such as polyethylene glycol (PEG) with different molecular weights [24]. However, after immersing the gelcast parts in PEG, only some part of water in the gelcast parts was removed and then the PEG immersion needed another further drying stage. It meant that the liquid desiccant functioned as only the early stage of de-watering.

In this work, a promising, alternative liquid for drying the agar-gelled Al_2O_3 tubes was proposed for achieving the economical fabrication and solving the problem of long drying period. Acetone was used as the liquid agent for drying and then enable to reduce the drying time. The effects of periods of different immersion time from 0 to 50 h on the net shape and shrinkage of Al_2O_3 tubes after drying were observed. After sintering, the pore size distribution was investigated for the possibility of application as tubular Al_2O_3 membrane.

2. Experimental

2.1 Preparation of gelcasting mixture

The flow chart of fabricating the Al_2O_3 tubes by agar gelcasting and then acetone-assisted drying was displayed in Fig. 1. The starting materials consisted of two sizes of Al_2O_3 powder (A-321, 14.33 μm, local supplier, Thailand and TM-DAR, 0.167 μm, Taimicron, Taimei Chemicals co., Ltd., Japan). The proportion of A-321 to TM-DAR powder was fixed at 80:20 for creating the pore size in the range of microfiltration [25]. The TM-DAR powder was used for yielding high strength using low sintering temperature of 1350°C. The Al_2O_3 slurry with 50 vol.% solid loading was ball milled for 2 h in a HDPE bottle. Sodium salt of polyacrylic acid (Na-PAA, Sigma-Aldrich) was used as a dispersant at 0.07 wt.% of solid loading. Subsequently, the Al_2O_3 slurry was warmed in a glass beaker at 70°C with a water bath. The glass beaker was covered with aluminum foil to prevent the evaporation of water in the Al_2O_3 slurry. In the preparation of agar solution separating from that of Al_2O_3 slurry, the agar powder was soaked in RO water for 5 min prior to being boiled to help in obtaining the clear agar solution with the concentration of 2 wt.%. The obtained agar solution was gently mixed with the warmed Al_2O_3 slurry before being maintained at the constant temperature of 70°C for gelcasting. The gelcasting step was shortly performed after obtaining the gelcasting mixture.

2.2 Forming of Al_2O_3 tube through agar gelcasting

To fabricate the Al_2O_3 tubes through agar gelcasting, a set of glass tubes was employed as molds as shown in Fig. 2. There were two glass tubes used for forming: the two opened-end (hollow) glass tube with 14-mm inner diameter, and the two closed-end glass tube with 10-mm outer diameter. It meant that the thickness of gelled tube equaled 2 mm. The closed-end one might be thinly coated with polyethylene glycol (molecular weight of 400) to prevent the attachment of gelled mixture during demolding. Prior to gelcasting, both the glass tubes were warmed in an oven at 70°C to prevent partially transforming from the mixture into gel. The warmed glass tubes were rapidly assembled to a specifically machined silicone parts as shown in Fig. 2. Additionally, synthetic clay was used for preventing the leakage of warmed mixture at the base of the assembled parts.

Shortly thereafter, the warmed gelcasting mixture was poured into the fixed glass tube. Subsequently, the warmed, small glass tube was rapidly fixed to the drilled middle hole of the silicone base [26]. An another

silicone hollowed by machining was quickly assembled for fitting the top-middle and outer glass tubes together. The prepared mixture was poured into the assembled molds at ~ 10–15 cm of glass tube length. After pouring for ~ 20-min ensuring completely the liquid-to-gel transformation, the outer glass tube was removed from the as-gelled Al_2O_3 tubes and then put left in air for about 30 min to loosely attach the as-gelled tubes to the surface of middle glass tube before being vertically immersed in acetone. The immersion of as-gelled tubes having also the middle glass tube was to prevent the collapse of tubes in the stage of gel.

Figure 3 showed the immersion of as-gelled Al_2O_3 tubes in acetone contained in glass cylinders tightly covered with thermoplastic film (Parafilm M). The periods of immersion time in acetone was varied from 0 to 50 h. After approaching each immersed periods, the acetone-rich, gelled tubes were removed from the glass cylinders and then the middle glass tube was immediately pulled out of the gelled tubes. Thereafter, the immediate evaporation of acetone in the gelled tubes rapidly occurred resulting in the drying in a short time.

2.3 Characterization

The weight loss percentages of gelling tubes during the evaporation of acetone were recorded for each immersed periods. The roundness of green tubes were calculated from the ratio of x-to-y axis diameters of green tubes measured from images from stereomicroscope. The percentages of drying shrinkage were calculated and then compared with the other types of gelling agents in gelcasting. The green tubes sintered at 1350°C for 1 h to provide the Al_2O_3 tubes with porous structure and mechanical strength. The sintering was performed in a tubular furnace (Henan Sante Furnace Technology Co., Ltd. Henan, China). After sintering, the percentages of shrinkage for each immersed periods in acetone were calculated. The tube porosity was examined by Archimedes' method (ASTM C373-88). The tube microstructure was observed with SEM (SEM-JSM5800LV, JEOL). The pore size distribution of sintered tubes was determined with Mercury Intrusion Porosimetry (Poremaster, Quantachrome Instruments). Hg contact angle and surface tension of 140° and 480 erg/cm^2, respectively, were used. A moving eleventh-point average was used in calculation.

3. Results And Discussion

3.1 Weight loss and drying time of gelling tube

Figure 4 showed the weight loss percentages during the drying of gelling Al_2O_3 tubes immersed in acetone at different periods of time. Apparently, the conventional air-drying tube displayed the tendency of gradually decreasing weight loss and spent 840 min (top abscissa) completing the drying. However, the tendency of weight loss for the acetone-immersing tubes indicated the marked decreases within early 40 min and then a slight decreases. The early marked decreases during drying implied that there was the sudden evaporation of acetone contained in the gelling Al_2O_3 tubes. Moreover, it was found that over the

progressive drying the gelling Al_2O_3 tubes were cool confirming that there was the continuous evaporation of acetone.

The inset of Fig. 4 displayed the weight-loss percentages of early 100 min for all the gelcast tubes. It was able to divide the tendency of weight losses into 3 characteristics according to the periods of immersing time: 1h, 5–30 h, and 40–50 h. Firstly, after 1 h of immersion the tendency of weight loss gradually decreased, rather similar to that of conventional air-drying tube. Secondly, the immersing time of 5–30 h demonstrated the weight loss of 27–28% at the early 30-min drying. Thirdly, at 30-min drying for the immersing time of 40 and 50 h, the weight losses were rather rapidly steady at 26 and 24.5%, respectively. The reduction in the weight losses from 28 to 24.5% was attributed to the calculation of weight loss percentages based on initial weight of gelling tubes containing only water inside. However, since the lost weights during rapid drying rooted from the acetone evaporation and the density of water (0.997 g/ml) is more than that of acetone (0.791 g/ml), the longer periods of acetone-immersing time led to more acetone replacement for water resulting in the lesser weight losses.

Figure 5 indicated the percentages of acetone replacing water in the gelled Al_2O_3 tubes at the different periods of immersing time obtaining from calculation based on the initial weight of gelling tubes just after removing from acetone. According to Fig. 4, the percentages of acetone replacement for water suggested the highly possible reasons for the weight loss divided into 3 characteristics. In comparison to Fig. 5, the acetone replacement percentages were also able to be divided into 3 ranges: < 30% for 1-h immersion, 30–50 % for 5- to 30-h immersion, and > 50% for 40- to 50-h immersion. When the acetone replacement was in the range of < 30%, the weight loss tendency was mainly dominated by the existence of water, i.e. the weight of gelling tube gradually decreased comparing with the other two ranges and then begin to be steady after 360-min drying. However, when the acetone replacement was in the range between 30 and 50%, the combined tendencies of weight loss from acetone and water were observed, noticeably for the initial 25 min, and then the period of 25–200 min, respectively. In other words, this range showed the two behaviors of weight loss in which rapid and then slow from acetone and water, respectively. For the acetone replacement in the range of > 50%, the rapidly acetone evaporation greatly dominated over the slowly water evaporation.

From Figs. 4 and 5, the immersion of agar-gelling tubes in acetone facilitated more rapid drying stage. The results of the behaviors of weight losses during drying confirmed the acetone replacement for water during the immersion of gelling tubes in acetone. The percentages of acetone replacement for water had the profound effect on the period of drying time.

3.2 Roundness of Al_2O_3 tubes

The comparison of the shape of green Al_2O_3 tubes between no immersion and 5-h immersion in acetone was shown in Fig. 6 (a) and (b), respectively. The cross section of gelling tube dried from no immersion noticeably deformed. Its cross section changed from circle to oval as well as the distortion along its length as shown in Fig. 6(a). On the other hand, after 5-h immersion its cross section remained unchanged as shown in Fig. 6(b). The unchanged cross-section proved the beneficial effect of immersion in acetone.

Figure 7 indicated the cross section of sintered tubes having the immersion in acetone at the different periods of time from 0 to 50 h. In order to be able to study the effect of acetone-assisted drying on the tube shape, the roundness of sintered-tube cross section was analyzed. The ratios of horizontal-to-vertical diameters of cross section was displayed in Table 1. It was noticeable that no immersion produced the tube with the smallest roundness. However, their roundness was considered to be rather equal for all the tubes with the immersion. As a result, the step of the immersion were highly beneficial for the drying of the agar gelcasting tubes with near-net shape.

Table 1
Roundness of sintered gelcast tubes having different periods of acetone-immersing time

Dimension	Acetone-immersing time (h)								
(mm)	0	1	5	10	15	20	30	40	50
a	12.24	12.679	13.226	12.975	12.627	12.991	12.884	13.000	12.830
b	11.39	12.785	13.226	12.871	12.754	12.928	12.946	12.872	12.766
Roundness (a/b ratio)	1.08	0.992	1.000	1.008	0.990	1.005	0.995	1.010	1.005
Note: a = Horizontal, outer diameter, b = Vertical, outer diameter									

In addition, It was found that the cycle number of immersion affected the performance of acetone replacement for water. In other words, the acetone replacement during the immersion was less and less when the acetone was repeatedly used. Obviously, for 500-ml acetone and only one gelling tube it was suitable for only 4-time immersion. For the immersion more than 4 times, it appeared to not allow the gelling tubes to be dried rapidly as well as the fresh acetone. The > 4-time immersion produced the tubes with unacceptable distortion. The distortion might resulted from the acetone-water concentration gradient decreased when the acetone was reused. Therefore, the acetone was usable for a limited number of immersion. The results suggested that the water staying inside the gelling tubes diffused into the surrounding acetone during the immersing time, and vice versa. The interdiffusion between water and acetone was responsible for the dilution of acetone. Thus, the diffusion of acetone into the gelling tubes ended when their too low concentration gradient was approached. When the too low replacement of acetone for water occurred, the drying of gelling tubes was replaced by most of water evaporation.

Figure 8 showed the SEM images of both the surface and cross section of gelcast tubes with 5-h acetone immersion after both drying (a and a1) and sintering (b and b1). After drying, it was found that the alignment of Al_2O_3 particles at the surface occurred as shown in Fig. 8(a). However, there was no aligned Al_2O_3 particles for the cross section as shown in Fig. 8(a1). Moreover, both the microstructures after drying was the same as those after sintering as shown in Fig. 8(b) and (b1). At the surface, the alignment of Al_2O_3 particles being in all the same direction was attributable to behavior of particles pulled out of the glass mold. The step of de-molding of gelling tubes was similar to the extrusion process of ceramic tubes. The de-molding resulted in the preferred orientation of Al_2O_3 particles at the surface of Al_2O_3 tubes [1, 26–27].

Whereas, at the cross section the alignment of Al_2O_3 particles was apparently random to the surface of glass mold. However, it was worth reminding that the large Al_2O_3 particles of A-321 had the shape of platelet, thereby able to be arranged in a certain direction.

Furthermore, the microstructures of dried tubes seemed denser than those of sintered tubes. The denser microstructures could result from the existence of dried agar strongly bound to the Al_2O_3 particles. The dried agar functioning as a binder offered the advantage of high green strength. After sintering, the microstructures of sintered tubes indicated the porous structure due to sintering effect as shown in Fig. 8(b) and (b1).

3.3 Shrinkage, porosity and pore size of gelcast Al_2O_3 tubes

The percentages of linear shrinkage during drying of the gelcast tubes as a function of elapsed time were shown in Fig. 9(a); while, the total linear shrinkage as a function of the acetone-immersing time was shown in Fig. 9(b). The tendency of linear shrinkage between the conventional air-drying and the acetone-assisted drying clearly different. The air drying spent 420 min approaching no shrinkage gradually. In contrast, the acetone-assisted drying spent approximately 20–50 min approaching no shrinkage. Moreover, the longer the acetone-immersing time, the shorter the spending time in approaching no shrinkage. The results of shrinkage confirmed the benefit of acetone-assisted drying leading to the rapidly dried tubes with near-net shape. Furthermore, the total drying shrinkage significantly decreased from 12.1 to 4.7% for the air drying and the drying having the step of immersing in acetone for 50h, respectively. The total firing shrinkage slightly increased from 2 to 2.6% from no immersion to 50h immersion in acetone. All the results of shrinkage suggested that the microstructure and pore size between no immersion and the immersion were likely to differ with each other due to the significant effect of drying shrinkage.

It was interesting to compare the drying shrinkage of agar-based gelcasting in this work with the other polymer-based gelcasting system as shown in Table 2. In this work, although the agar gelcasting with 50 vol.% solid loading and 0.5 wt.% of agar was used, the air-drying shrinkage was the highest (12.1%). The highest shrinkage was attributable to both the characteristics of agar macromolecules during their gel formation creating the network of wall and internal cavity and its high molecular weight. Moreover, the high shrinkage resulted from agar acting as flocculating agent or bridging flocculation [7, 29]. In other words, agar was adsorbed on each adjacent particles of Al_2O_3 forming polymer bridges. The polymer bridges acted as a barrier preventing the close contact of Al_2O_3 particles. In addition to the agar properties, the shape and size of Al_2O_3 particles had significant effect on asymmetric shrinkage of the gelcast Al_2O_3 tubes as well [30].

Table 2
Comparison of shrinkage percentages among various kinds of gelling agent in gelcasting system

Gelling agent (as % of solid loading)	Molecular weight (g/mol)	Solid loading (vol. %)	Drying shrinkage (%)	Drying method	References
Agar and galactomannan = 80:20 (0.2–0.6 wt%)	336.33	40	3.9–6.1	Air drying	[7]
	and 504.4	50	0.9–2.6		
		60	0.4–1.3		
AM/MBAM (17 wt%)	71.08 and 154.17	55	2.8	95% relative humidity	[8]
AM/MBAM (17 wt%)		60	0.53		
AM/MBAM (not shown)		40	6.0	PEG 1000 (60 wt% in water)	[22]
Agarose (0.5 wt%)	306.267	39	6.0	Air drying	[28]
Agar (0.5 wt%)	336.33	50	12.1	Conventional air-drying	This work
			4.7	Acetone-assisted drying for 50h	

Figure 10 showed the apparent porosity, water absorption and bulk density of the sintered gelcast tubes as a function of the periods of acetone-immersing time. The apparent porosity of gelcast tubes increased from 40 to 44% when the acetone-immersing time increased from 0 to 5 h. After the immersing time of ≥ 5 h, their porosity was constant at 44% on average. The water absorption indicated the same trend as the porosity. The water absorption increased from 17 to 20% while the immersing time reached 5 h. Moreover, the bulk density decreased from 2.35 to 2.15 g/cm^3 during the early 5 h of immersion. Therefore, those tendencies were divided into 2 main ranges on the basis of immersing time: the immersion periods of ≤ 5 h and > 5 h. Additionally, it was found that those tendencies were the same as the linear drying shrinkage.

Figure 11 displayed the pore size distribution within the sintered Al_2O_3 tubes characterized with MIP. No immersion in acetone displayed the feature of narrow pore size distribution between 7.5 and 10 μm;

whereas the immersion characterized broad pore size distribution between 0.04 and 4.5 μm. The different results of pore size distribution were closely related to the markedly different evaporation rate of acetone and water during drying at room temperature. The evidence from the measurement of pore size distribution suggested that the average pore sizes were in the range of microfiltration (MF) membrane.

3.4 Microstructure of gelcast tubes after sintering

The SEM images of sintered tubes with the variation in acetone- immersing time of 0, 1, 5 and 50 h at outer surface and cross section were shown in Figs. 12 and 13, respectively. Noticeably, the gradual evolution of the microstructure of sintered tubes appeared in the way to the more open structure at both surface and cross section when the periods of acetone-immersing time increased. The more open structure corresponded with the decreasing density and increasing porosity as shown in Fig. 10. Therefore, the rapid drying from the high acetone volatility tended to offer the more open structure than the conventional air drying. It suggested that if the denser structure of gelcast tubes was required, it needed the higher sintering temperature than the usual.

4 Conclusion

The alternative drying method of Al_2O_3 tube fabricated by agar gelcasting was successfully applied to this work. Only the set of glass tubes was employed as mold for shaping the gelcast mixture into tube with the thickness of approximately 2 mm. The optimum acetone-immersing time of 50 h was needed for complete, rapid drying with no defect for green tube. The immersion of gelcast tubes in acetone led to the acetone-water interdiffusion resulting from the concentration gradient. The larger amount of acetone replacing water supported the uniformly rapid drying. The combination of agar gelcasting and acetone-immersing steps was the potentially pragmatic approach to fabricating the complex-shaped ceramics with near-net shape needless to use the highly sophisticated machines. The subsequent investigation of strength of sintered tubes needed to be conducted in the future work for membrane application.

Declarations

5. Acknowledgement

The authors would like to thank Thailand Graduated Institute for Science and Technology (TGIST) for financial support [grant number: TG-33-18-61-024M]. Additionally, this work was supported by the government budget of Prince of Songkla University [grant number: SCI6201046S]. In addition, we greatly appreciate for providing the high quality tubular furnace with low cost for sintering in this work from Henan Sante Furnace Technology Co., Ltd. Henan, China.

References

1. Rice RW (2003) Ceramic fabrication technology. Marcel Decker, New York

2. Bresciani A (2007) Shaping in ceramic technology – an overview. In: Händle F (ed) Extrusion in ceramics. Springer-Verlag Berlin Heidelberg, New York, pp 13–33
3. Chartier T (2007) Ceramic forming processes. In: Boch P, Nièpce J-C (eds) Ceramic Materials: Processes, Properties and Applications. Wiley-ISTE, London, pp 123–198
4. Montanaro L, Coppola B, Palmero P et al (2019) A review on aqueous gelcasting: A versatile and low-toxic technique to shape ceramics. Ceram Int 45:9653–9673
5. Wu H, Li D, Tang Y et al (2009) Rapid fabrication of alumina-based ceramic cores for gas turbine blades by stereolithography and gelcasting. J Mater Process Tech 209:5886–5891
6. Gilissen R, Erauw JP, Smolders A et al (2000) Gelcasting. a near net shape technique. Mater Design 2:251–257
7. Olhero SM, Tarì G, Coimbra MA et al (2000) Synergy of polysaccharide mixtures in gelcasting of alumina. J Eur Ceram Soc 20:423–429
8. Young AC, Omatete OO, Janney MA et al (1991) Gelcasting of alumina. J Am Ceram Soc 74:612–618
9. Omatete OO, Janney MA, Nunn SD, Gelcasting (1997) From laboratory development toward industrial production. J Eur Ceram Soc 17:407–413
10. Janney MA, Omatete OO, Walls CA et al (1998) Development of low-toxicity gelcasting systems. J Am Ceram Soc 81:581–591
11. Tallon C, Jach D, Moreno R et al (2009) Gelcasting of alumina suspensions containing nanoparticles with glycerol monoacrylate. J Eur Ceram Soc 29:875–880
12. Wan W, Yang J, Zeng J et al (2014) Effect of solid loading on gelcasting of silica ceramics using DMAA. Ceram Int 40:1735–1740
13. Cai K, Huang Y, Yang J (2005) Alumina gelcasting by using HEMA system. J Eur Ceram Soc 25:1089–1093
14. Kokabi M, Babaluo AA, Barati A (2005) Gelation process in low-toxic gelcasting systems. J Eur Ceram Soc 26:3083–3090
15. Xu J, Zhang Y, Gan K et al (2015) A novel gelcasting of alumina suspension using curdlan gelation. Ceram Int 41:10520–10525
16. Chen Y, Xie Z, Yang J et al (1999) Alumina casting based on gelation of gelatin. J Eur Ceram Soc 19:271–275
17. Millán AJ, Nieto MI, Moreno R (2002) Near-net shaping of aqueous alumina slurries using carrageenan. J Eur Ceram Soc 22:297–303
18. Jia Y, Kanno Y, Xie Z-P (2002) New gel-casting process for alumina ceramics based on gelation of alginate. J Eur Ceram Soc 22:1911–1916
19. Santacruz I, Nieto MI, Moreno R (2005) Alumina bodies with near-to-theoretical density by aqueous gelcasting using concentrated agarose solutions. Ceram Int 31:439–445
20. Zhang Y, Xu J, Qu Y et al (2014) Gelcasting of alumina suspension using gellan gum as gelling agent. Ceram Int 40:5715–5721

21. Wang X-F, Peng C-Q, Wang R-C et al (2015) Liquid drying of BeO gelcast green bodies using ethanol as liquid desiccant. T Nonferr Metal Soc 25:2466–2472
22. Barati A, Kokabi M, Famili MHN (2003) Drying of gelcast ceramic parts via the liquid desiccant method. J Eur Ceram Soc 23:2265–2272
23. Hammel EC, Pettaway K, Ichite T et al (2019) Towards optimization of the osmotic drying process of alumina-gelatin objects: Regression analysis and verification. Ceram Int 45:5223–5230
24. Hammel EC, Campa JA, Armbrister CE et al (2017) Influence of osmotic drying with an aqueous poly(ethylene glycol) liquid desiccant on alumina objects gelcast with gelatin. Ceram Int 43:16443–16450
25. Chee DNA, Ismail AF, Aziz F et al (2020) The influence of alumina particle size on the properties and performance of alumina hollow fiber as support membrane for protein separation. Sep Purif Technol 250:117147
26. Kaemkit R, Vichaphund S, Lertwittayanon K (2020) Fabrication of Low Cost Alumina Tube through Agar Gelcasting for Membrane Microfiltration. AMST 24:47–57
27. Wu X, Chen I (1992) Hot Extrusion of Ceramics. J Am Ceram Soc 75:1846–1853
28. Adolfsson E (2006) Gelcasting of Zirconia Using Agarose. J Am Ceram Soc 89:1897–1902
29. Shanefield DJ (1995) Organic additives and ceramic processing with applications in powder metallurgy, ink and paint. Springer Science + Business Media, New York
30. Besendörfer G, Roosen A (2008) Particle Shape and Size Effects on Anisotropic Shrinkage in Tape-Cast Ceramic Layers. J Am Ceram Soc 91:2514–2520

Figures

Fig. 1

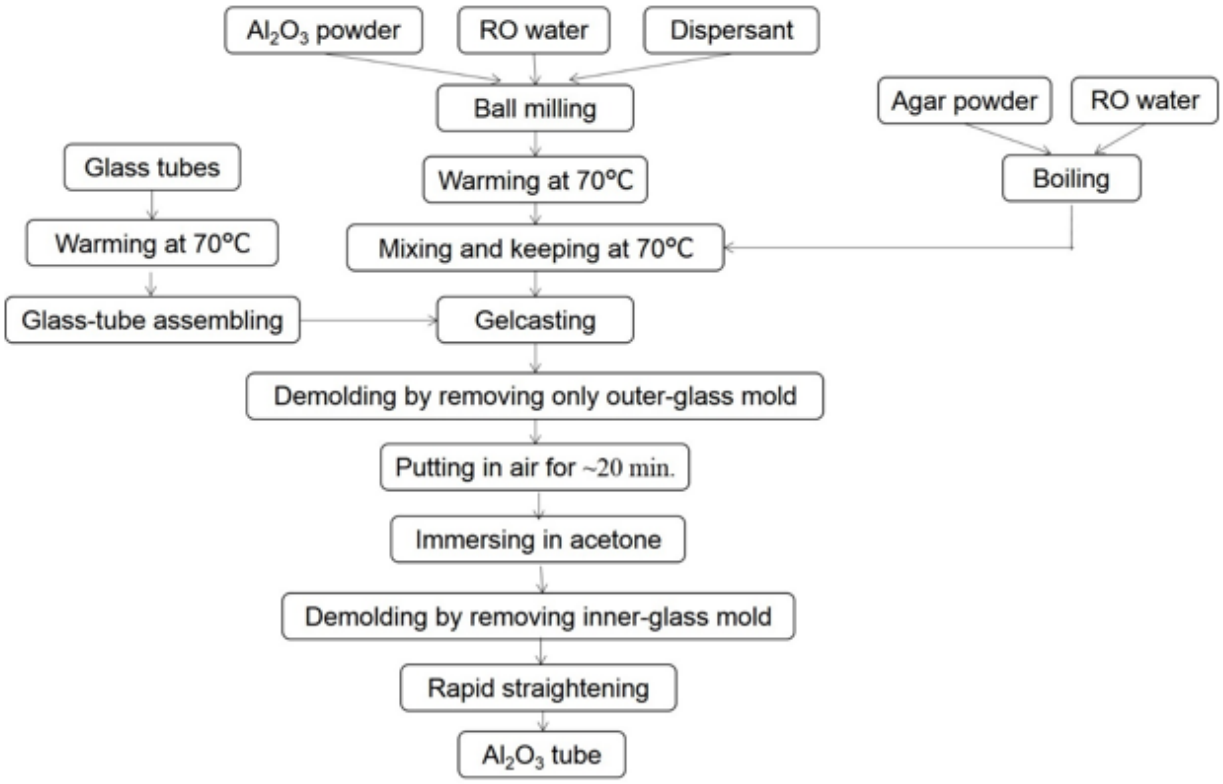

Figure 1

Flow chart of fabricating the Al2O3 tubes through the combined steps of agar gelcasting and acetone-assisted drying.

Fig. 2

Figure 2

As-gelled Al2O3 tubes and assembly of glass-tube mold.

Fig. 3

Figure 3

Immersion of as-gelled Al2O3 tubes in acetone

Fig. 4

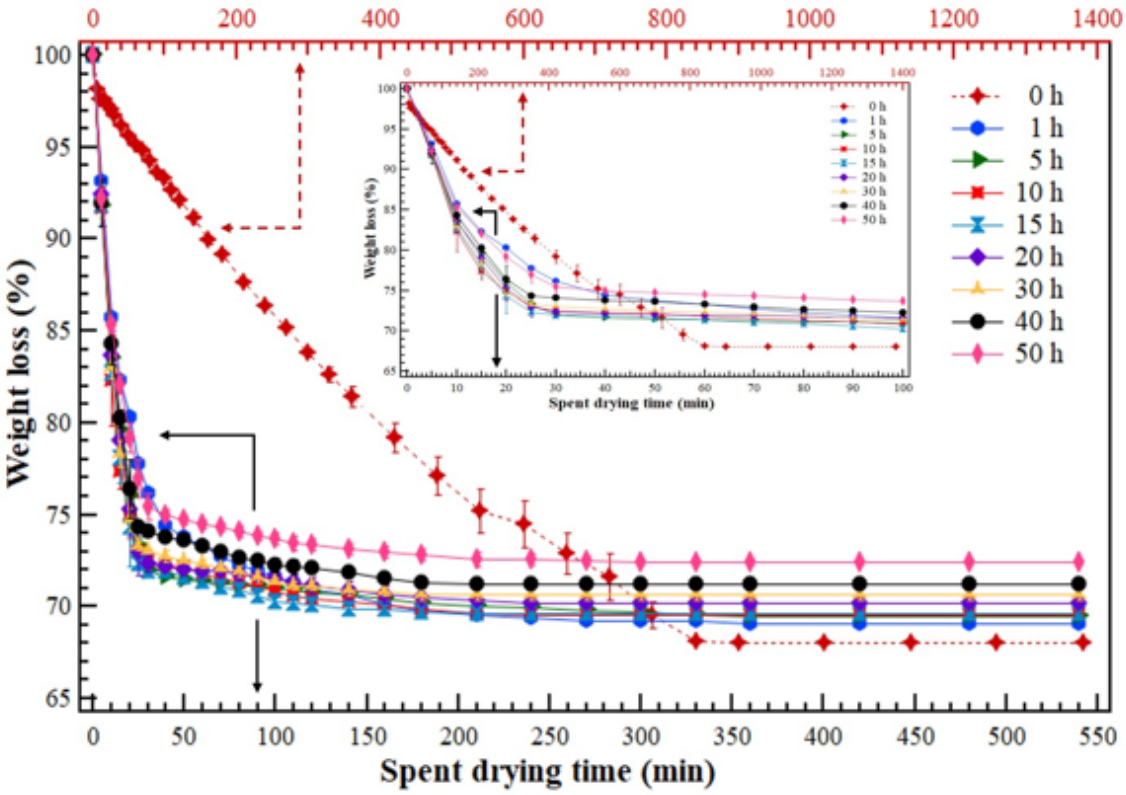

Figure 4

Weight loss percentages during drying of the gelled Al2O3 tubes immersed in acetone at 0, 1, 5, 10, 15, 20, 30, 40, 50h.

Fig. 5

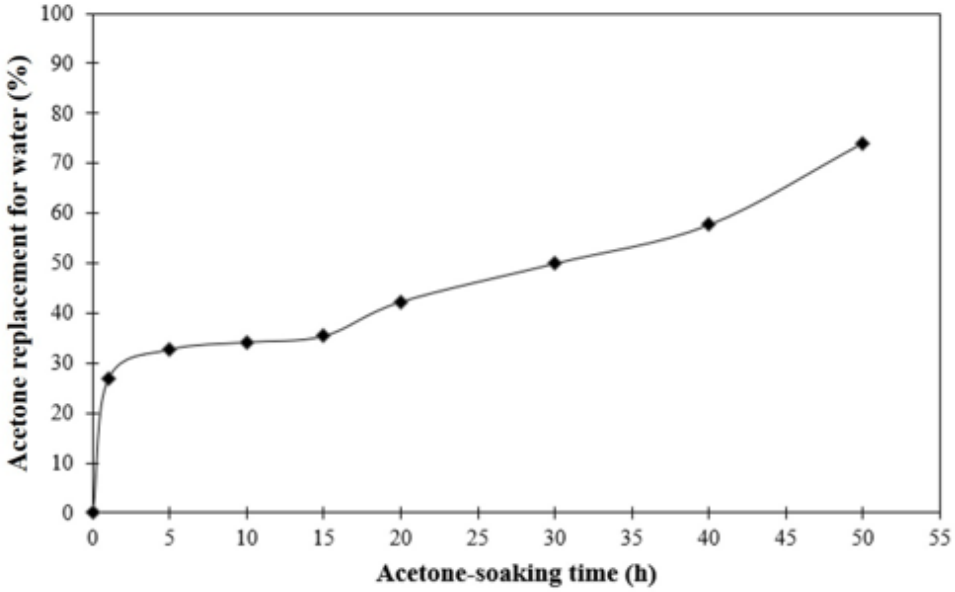

Figure 5

Percentages of acetone replacement for water in the gelled Al2O3 tubes immersed in acetone at 0, 1, 5, 10, 15, 20, 30, 40, 50h.

Fig. 6

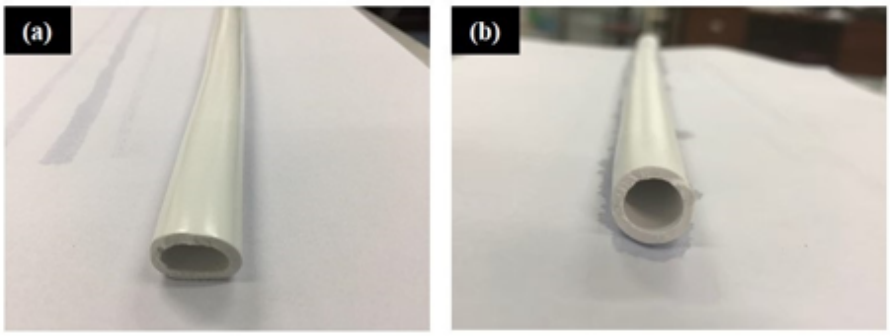

Figure 6

Green Al2O3 tubes using (a) conventional air-drying and (b) 5 h immersion in acetone.

Fig. 7

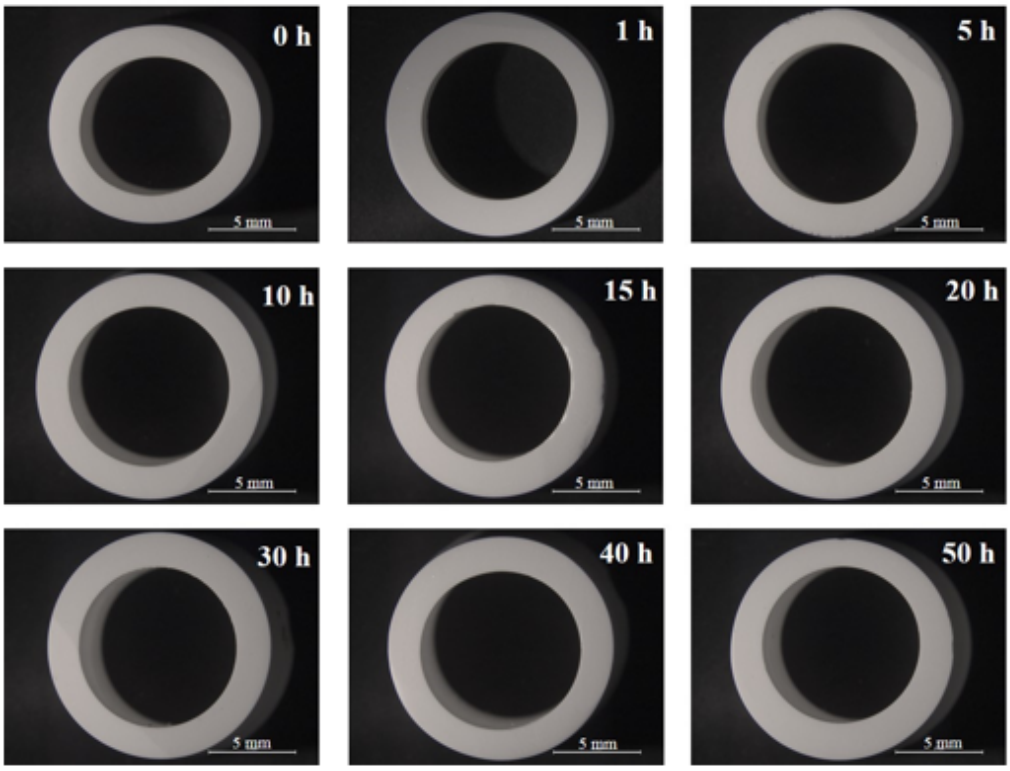

Figure 7

Cross-section images of the sintered Al2O3 tubes immersed in acetone at 0, 1, 5, 10, 15, 20, 30, 40, 50h.

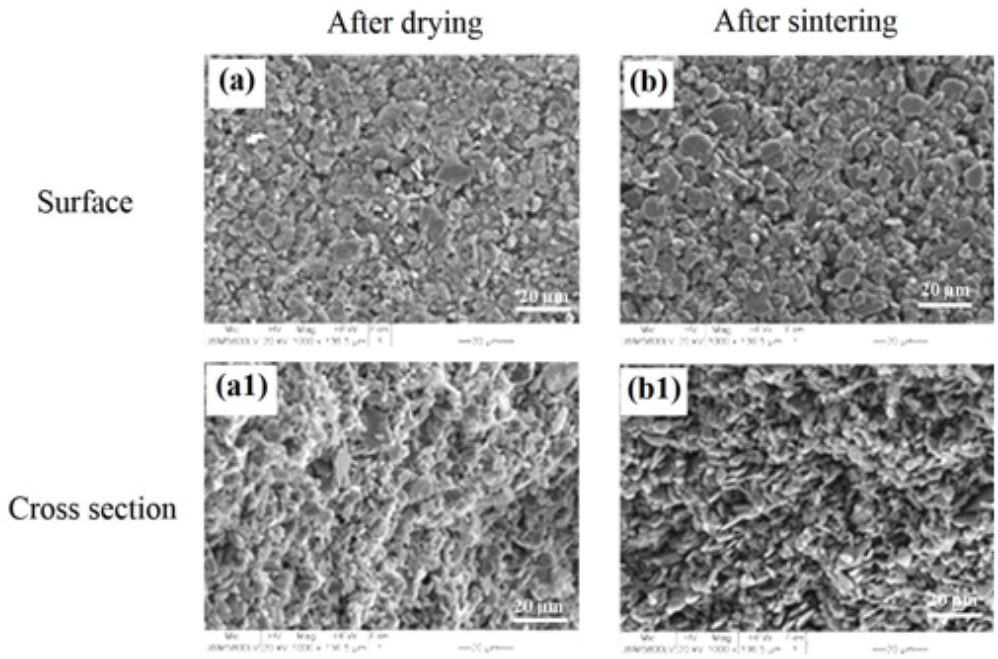

Figure 8

SEM images of Al2O3 tubes after drying using 50 h-acetone soaking at (a) surface and (a1) cross section, and after sintering at 1350°C at (b) surface and (b1) cross section.

Fig. 9

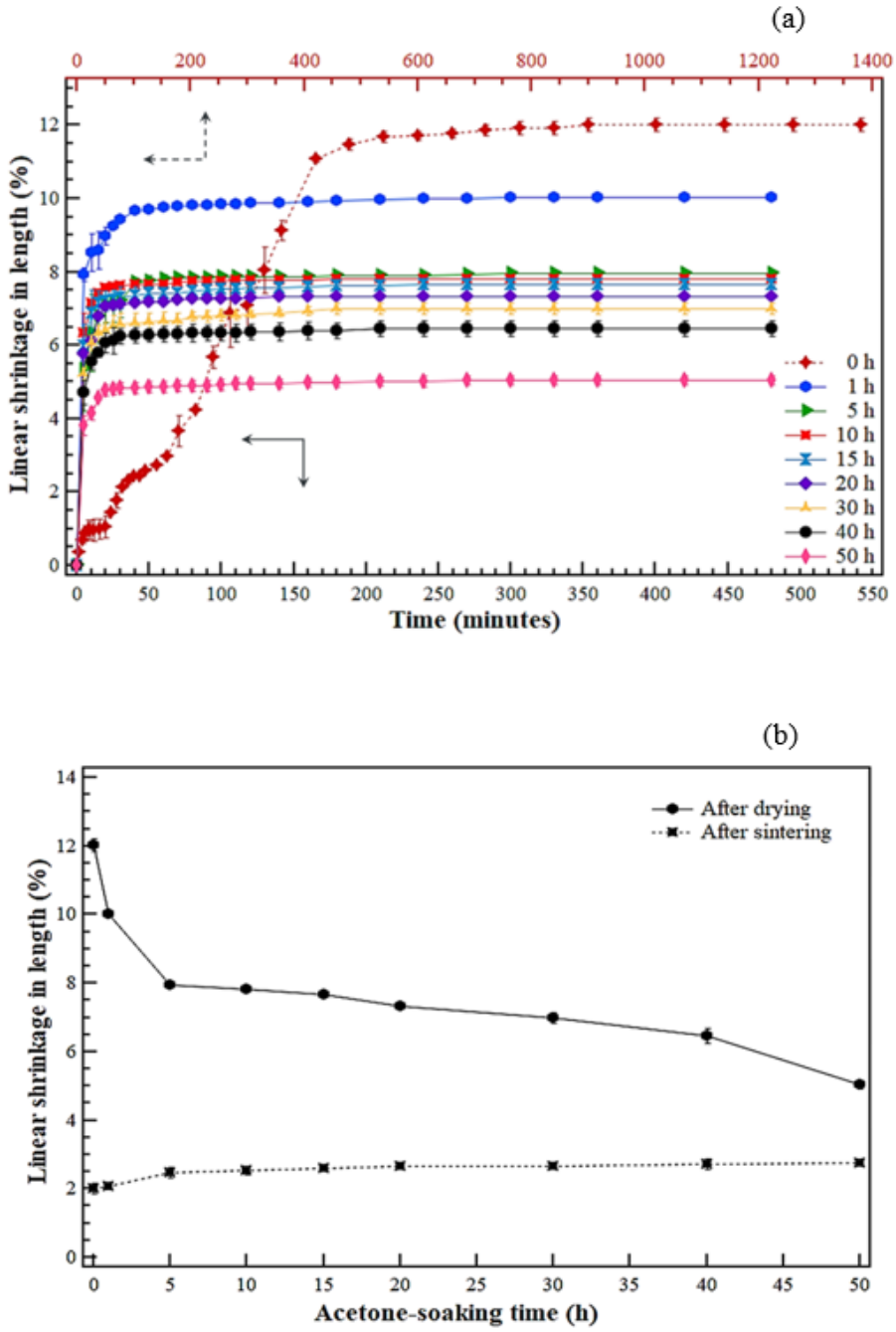

Figure 9

Relationship between (a) the percentages of linear shrinkage and passed time during drying, and (b) the average total linear shrinkage and different acetone-immersing time, for the as-gelled Al2O3 tubes.

Fig. 10

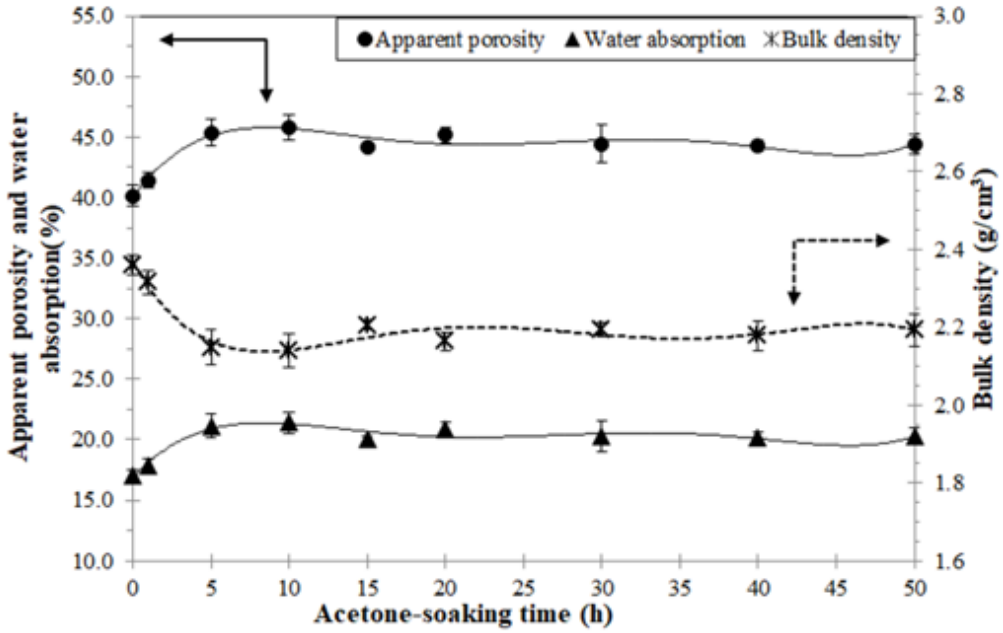

Figure 10

Apparent porosity, water absorption and bulk density of sintered Al2O3 tubes as a function of acetone-immersing time from 0 to 50 h.

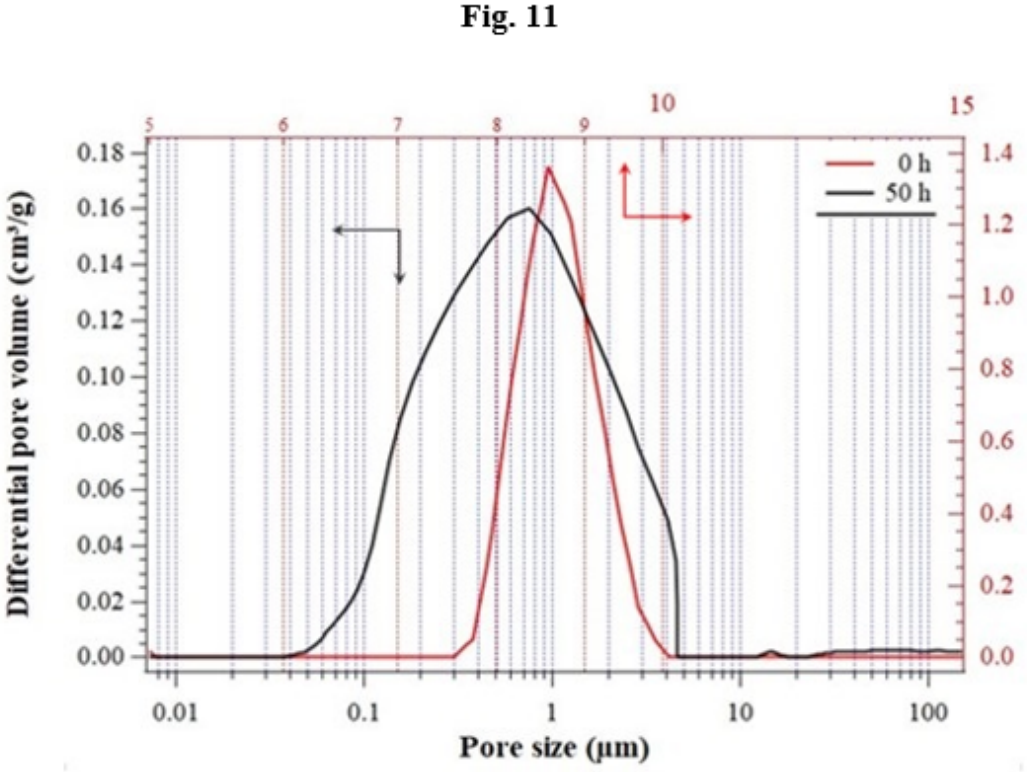

Figure 11

Pore size distribution of the gelcast tubes with acetone-immersion at the time of (a) 0 h (red grid line) and (b) 50 h (black grid line).

Fig. 12

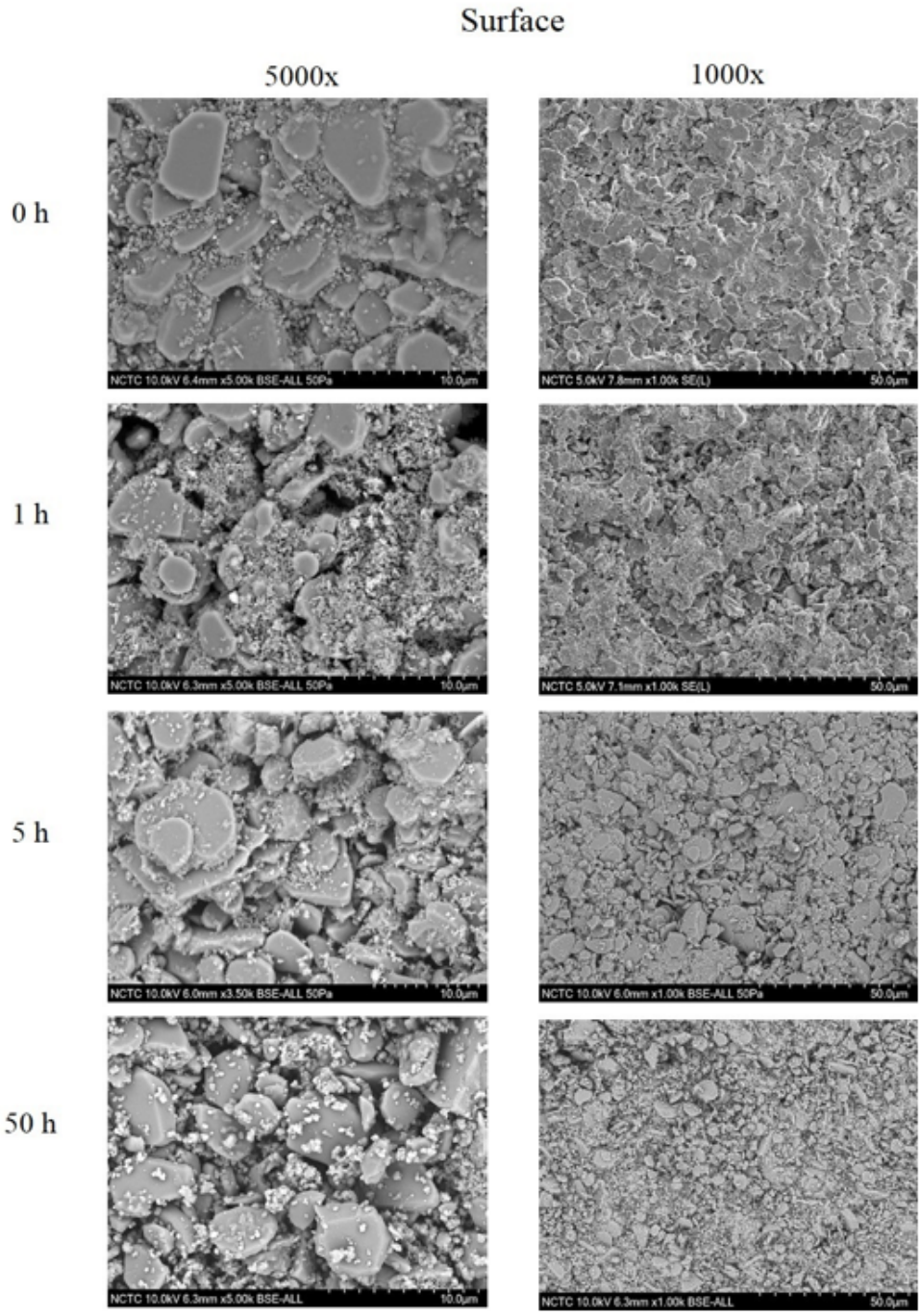

Figure 12

SEM images of sintered Al2O3 tubes at surface with acetone-immersing time of (a) 0, (b) 1, (c) 5 and (d) 50 h at the magnification of 5000x (left) and 1000x (right).

Fig. 13

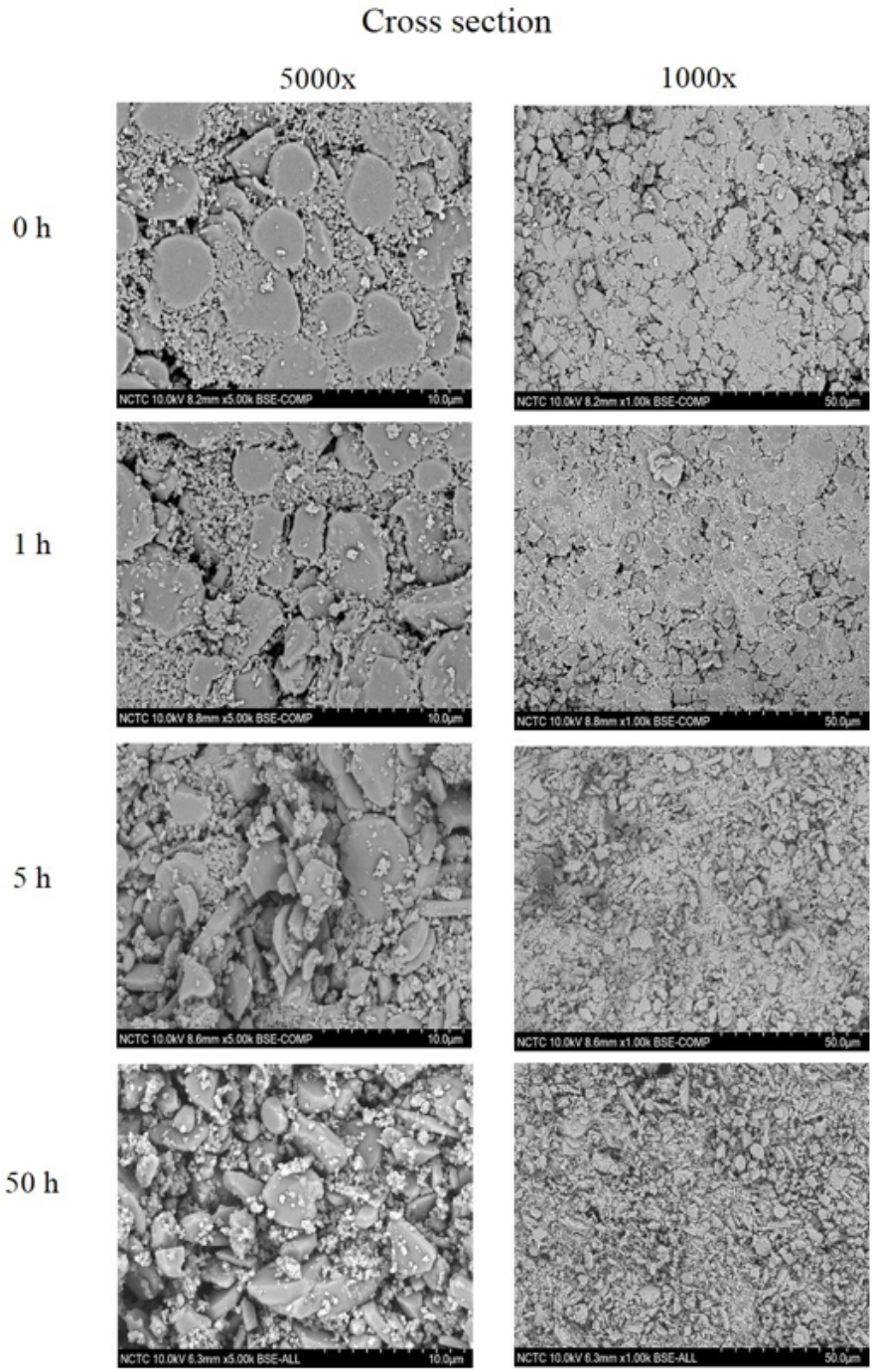

Figure 13

SEM images of sintered Al2O3 membrane tubes at cross section after polishing with acetone-immersing time of (a) 0, (b) 1, (c) 5 and (d) 50 h at the magnification of 5000x (left) and 1000x (right).